Real-time influence of intracellular acidification and NHE1 inhibition on in-cell pyruvate metabolism in the perfused mouse heart

Short title: **Cardiac acidification & real-time enzyme activity**

David Shaul [1, 2], Naama Lev-Cohain [1], Gal Sapir [1, 2], Jacob Sosna [1],
J. Moshe Gomori [1], Leo Joskowicz [3], and Rachel Katz-Brull [1, 2*]

[1] Department of Radiology, Hadassah Medical Organization and Faculty of Medicine, Hebrew University of Jerusalem, Israel

[2] The Wohl Institute for Translational Medicine, Hadassah Medical Organization, Jerusalem, Israel

[3] School of Computer Science and Engineering, The Hebrew University of Jerusalem, Israel

* Corresponding author

Supporting Information

- For Review –

Figure S1. The reactions leading to the intracellular acidification following an NH_4Cl prepulse and removal and the time of pyruvate metabolism recordings.

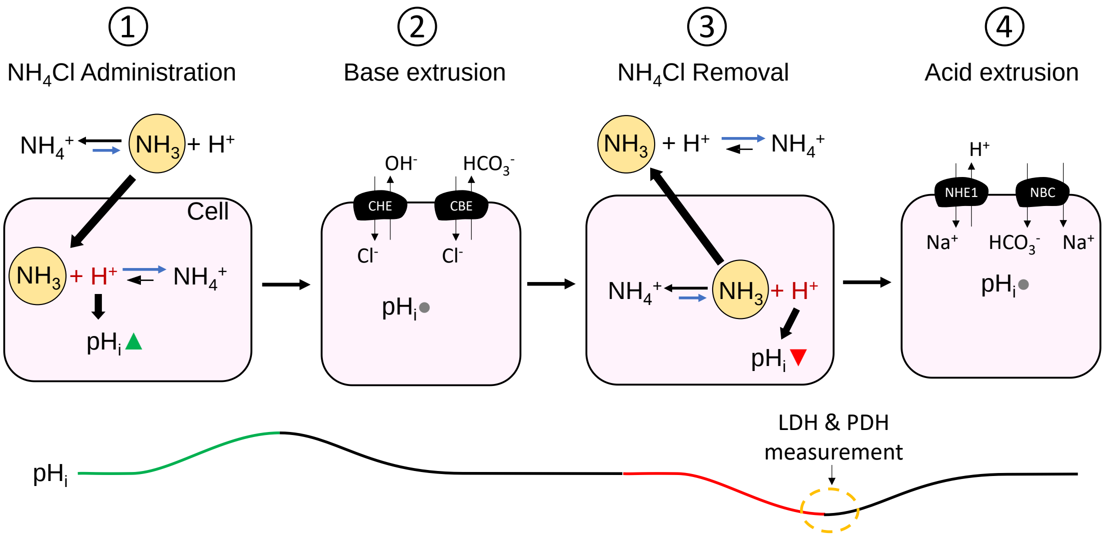

1) Free ammonia is formed in equilibrium with the NH_4Cl that is added to the perfusing medium. The ammonia passively enters the cell, where an equilibrium with NH_4Cl will eventually occur as well. In the process, hydronium ions are absorbed leading to temporary intracellular alkalinization.

2) The membrane-bound pH regulators, Cl^-/OH^- exchanger (CHE) and Cl^-/HCO_3^- exchanger (CBE) normalize the pH_i by transporting OH^- and HCO_3^- out of the cell, respectively.

3) Removal of ammonium-chloride from the buffer drives ammonia out of the cell due to the formation of a concentration gradient, which causes a temporary hydronium ions excess and intracellular acidification. During this phase, the hyperpolarized [1-^{13}C]pyruvate was injected to the heart and the LDH and PDH activities were measured.

4) The membrane bound pH regulators, Na^+/H^+ (NHE) and Na^+/HCO_3^- co-transporter (NBC) normalize the pH_i by transportation of H^+ out of the cell and HCO_3^- into the cell, respectively.

Figure S2. The reverse operations of NHE1 on the plasma membrane and the mitochondrial membrane.

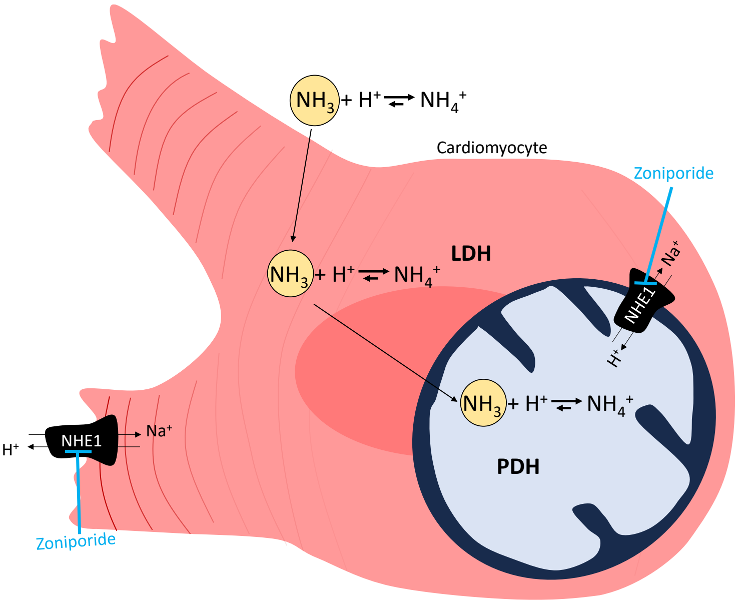

The various ammonia and ammonium equilibria that may form during an NH_4Cl pre-pulse are shown.

Figure S3. The content of PCr and ATP following NHE1 inhibition.

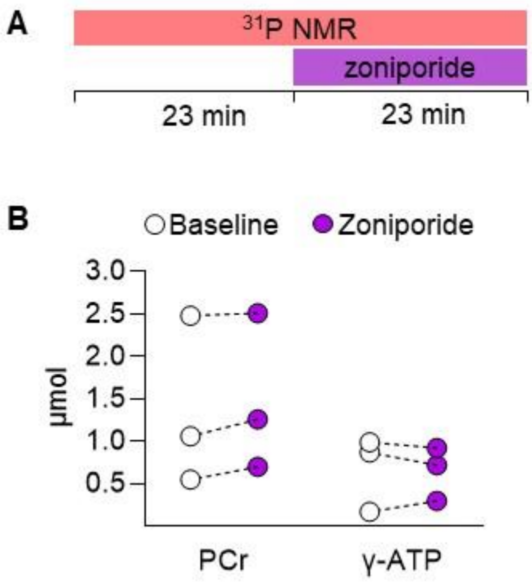

The content of cardiac PCr and γ-ATP before (baseline, empty circles) and during perfusion with 1 µM zoniporide (full circles). Each data point was acquired for 23 min using ^{31}P NMR spectroscopy. Each data point represents a single measurement in a single heart. Dashed lines connect data points from the same heart. There was no change in the PCr or ATP content due to the perfusion with zoniporide alone (Paired, two-tailed Student's *t*-test). This study was carried out in experimental Group 3 (see Figure 2 in the text).

Figure S4. Comparison of LDH and PDH rates with and without normalization to ATP content.

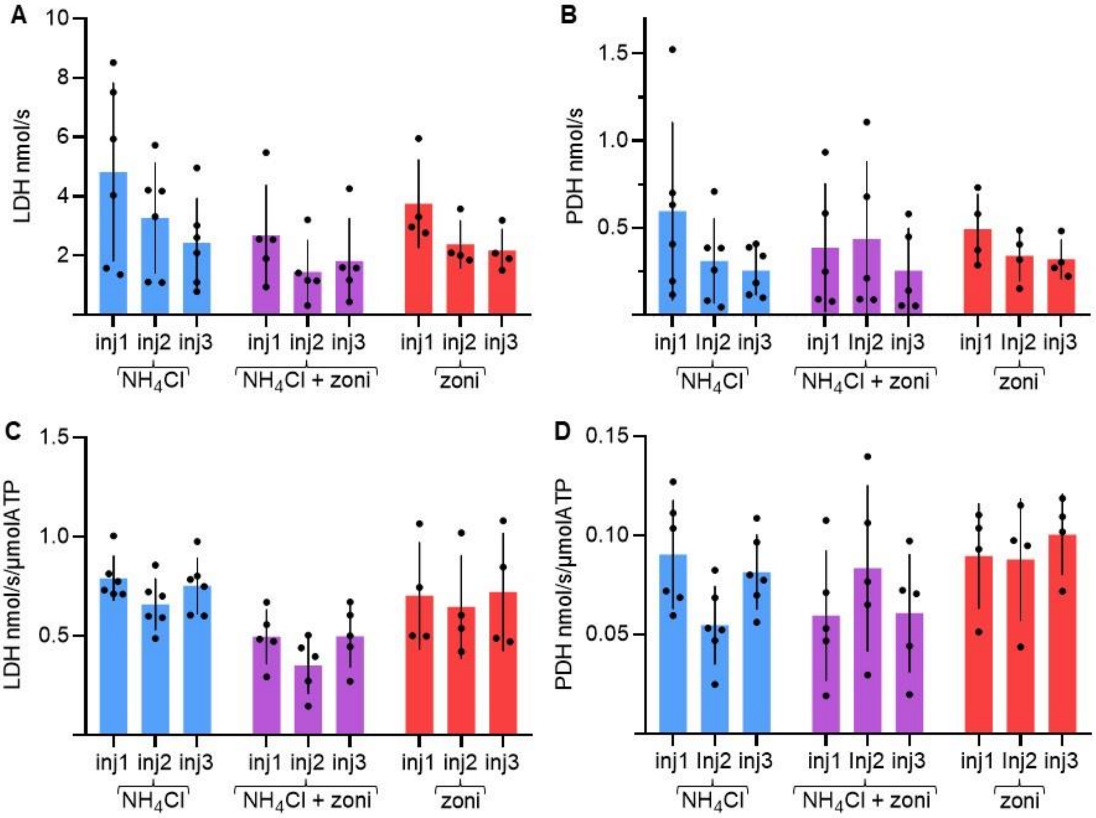

LDH and PDH rates without (A and B, respectively) and with (C and D, respectively) normalization to the ATP content. C and D are replication of Figure 9A and 9B, respectively.

zoni, zoniporide.

Figure S5. The calculation of ΔDO and its time course in each heart under control and intracellular acidification conditions, with and without NHE1 inhibition.

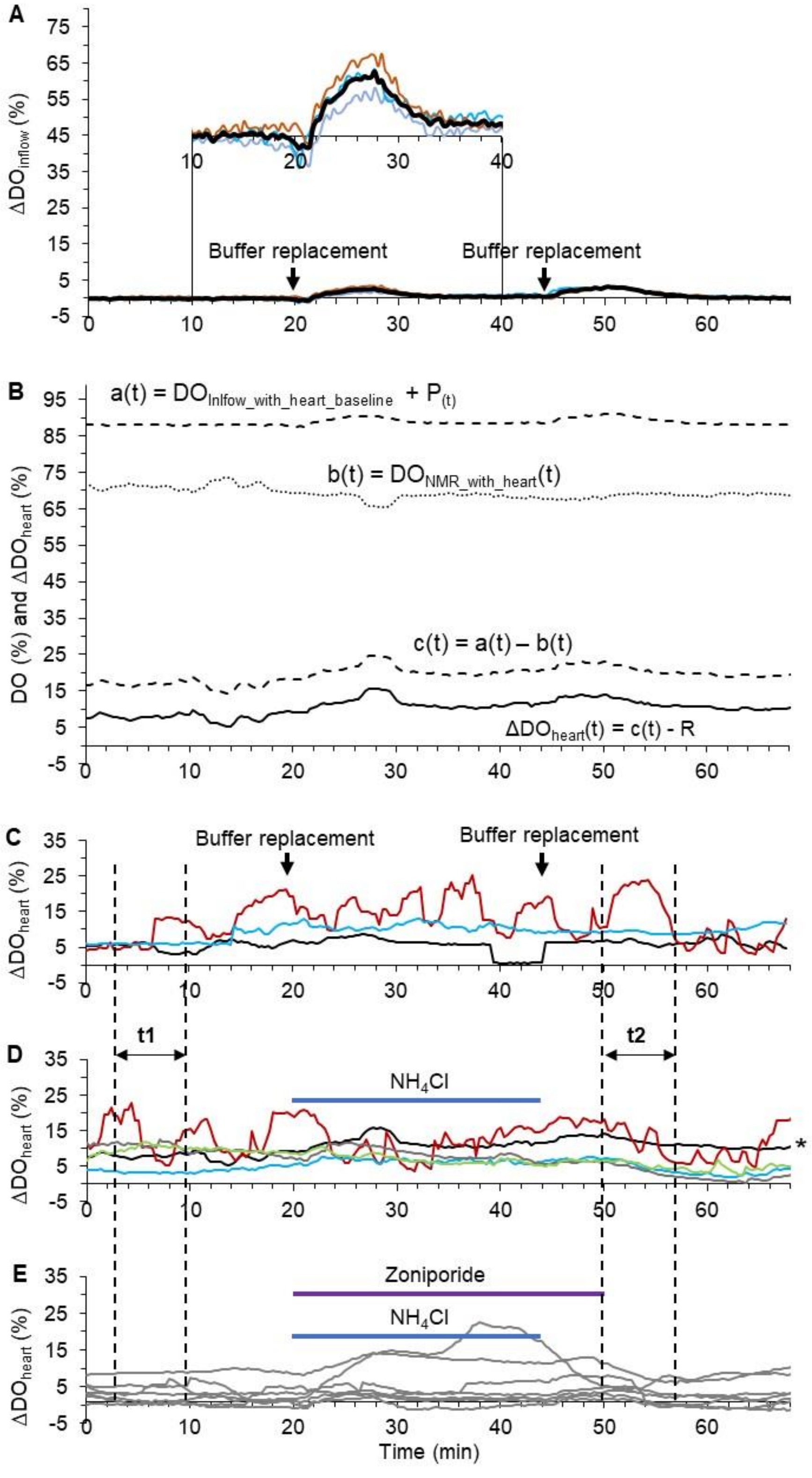

A) Changes in DO in the inflow line during buffer replacement. Each thin line represents an individual experiment (n=3) in which a new bottle of fresh KH buffer was connected to the perfusion system. This was done to control for changes in DO that were due to buffer replacement. The thick black line represents the averaged value of the three experiments, and it is termed here $P_{(t)}$. Inset, 15 times enlargement of this behavior for the first buffer replacement – for clear visualization of the various lines.

B) The steps of ΔDO calculation in a typical experiment. These steps are described by Equations S5 and S6.

The upper dashed line, (marked ‘a(t)’), is $P_{(t)}$ plus the baseline DO in the inflow line with the heart connected ($DO_{inflow\_with\_heart\_baseline}$). In this specific experiment $DO_{inflow\_with\_heart\_baseline}$ was 88.0 %.

The dotted line, (marked ‘b(t)’), is the DO that was measured inside the NMR tube that contained the heart.

The lower dashed line, (marked ‘c(t)’) is the subtraction of b(t) from a(t).

The solid line, (marked ‘$\Delta DO_{heart}(t)$’) is calculated by subtracting R, (Equation S5), from c(t). In this specific experiment, the R was 9.1 %.

C, D, E) Each line represents a ΔDO_{heart} time course for an individual heart.

C) The measurements were done in Group 1, under control conditions (n=3), in which an identical buffer, that did not contain NH_4Cl nor zoniporide, was used for the buffer replacement procedure (Solution 1). This refers to the first hour of the perfusion of three hearts in group 1. The recording from the next hour, in which the NH_4Cl pre-pulse was administered and removed is described in D.

D) The measurement was done in Group 1, during the NH_4Cl pre-pulse (n=5). The KH buffer was replaced with the same buffer that contained NH_4Cl (solution 2). The bold black line that is marked by an asterisk is the same experiment that is presented in B (also black line). The black, light blue, and dark red lines are from the same animals that are presented in C (with the same line color). However, the data shown in D and C are from different time durations during the experiment.

E) The measurement was done in Group 2, during the NH_4Cl pre-pulse with the zoniporide NHE1 inhibition (n=7). The KH buffer was replaced with the same buffer that contained NH_4Cl and zoniporide (solution 3).

The dashed lines mark the start and end of the time durations for which the ΔDO_{heart} was checked for significance of change. The time durations marked t1 and t2, (7 min each, from 3-10 min and from 50-57 min, respectively), represent the durations for which ΔDO_{heart} was measured under baseline perfusion conditions and under intracellular acidification conditions, respectively. For each individual experiment in C, D and E, the data points in t1 and in t2 were averaged. These averaged values were tested for significance with two-tailed, paired, Student's *t*-tests within each group. We did not find significant changes between t1 and t2 in C, D, and E.

Figure S6. Illustration of the proposed mechanism for in-cell LDH and PDH activity changes further to intracellular acidification that results from an NH_4Cl prepulse and NHE1 inhibition.

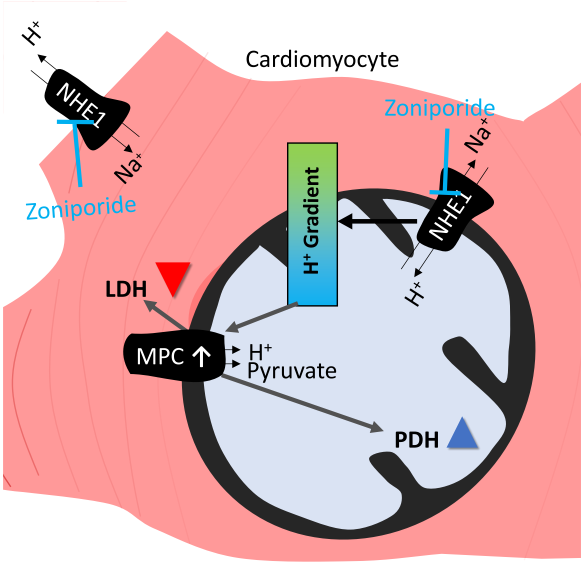

Table S1. Individual values of LDH and PDH activity and ATP content in each of the hearts in Groups 4-6.

	Animal No.	**LDH (nmol/s)**			**PDH (nmol/s)**			**γ-ATP (μmol)**		
		Inj 1	**Inj 2**	**Inj 3**	**Inj 1**	**Inj 2**	**Inj 3**	**Inj 1**	**Inj 2**	**Inj 3**
Group 4 NH_4Cl pre-pulse	1	5.9	4.2	2.6	0.4	0.3	0.2	5.9	4.9	3.3
	2	1.4	1.1	0.8	0.2	0.1	0.1	1.9	1.5	1.1
	3	4.0	3.3	2.1	0.6	0.4	0.3	5.7	5.6	3.5
	4	1.6	1.1	1.1	0.1	0.0	0.1	1.9	1.8	1.4
	5	7.9	4.2	3.0	1.4	0.7	0.4	12.0	8.6	5.0
	6	7.5	5.7	5.0	0.7	0.4	0.4	9.7	8.2	5.1
Group 5 NH_4Cl pre-pulse + NHE1 inhibition	7	2.6	1.4	1.6	0.2	0.2	0.1	5.3	3.2	3.2
	8	2.5	1.2	1.6	0.9	1.1	0.6	8.7	7.9	6.0
	9	1.9	1.2	1.2	0.1	0.1	0.1	4.0	3.0	2.7
	10	0.9	0.3	0.4	0.1	0.1	0.1	1.7	1.2	0.7
	11	5.5	3.2	4.3	0.6	0.7	0.4	8.2	6.4	6.4
Group 6 NHE1 inhibition	12	6.0	3.6	3.2	0.6	0.4	0.3	5.6	3.5	3.0
	13	3.3	2.1	1.9	0.7	0.5	0.5	6.6	5.0	4.1
	14	3.0	2.0	2.1	0.4	0.3	0.3	4.0	3.3	2.5
	15	2.8	1.9	1.5	0.3	0.2	0.2	5.6	3.4	3.1

For each heart, LDH and PDH rates are specified for the three hyperpolarized [1-^{13}C]pyruvate injections (Inj). The first and the third injections (Inj 1 and Inj 3) were used as controls, while the second injection (Inj 2) was performed during the following conditions: Group 4, intracellular acidification that was performed using an NH_4Cl pre-pulse; Group 5, intracellular acidification using an NH_4Cl pre-pulse and NHE1 inhibition; Group 6, NHE1 inhibition only. The γ-ATP content was determined using the ^{31}P NMR signal of γ-ATP, acquired for 22.5 min immediately prior to each hyperpolarized [1-^{13}C]pyruvate injection.

Note S1. Materials and Methods

Chemicals

The OX063 radical (GE Healthcare, UK) was obtained from Oxford Instruments Molecular Biotools (Oxford, UK). [1-^{13}C] pyruvic acid was purchased from Sigma-Aldrich, (Rehovot, Israel) and from Cambridge Isotope Laboratories (Tewksbury, MA, USA). NaCl, KCl, NH_4Cl, D-glucose, $NaHCO_3$, $MgCl_2$, $NaH_2PO_4(2H_2O)$, $MgSO_4$, pyruvic acid, $CaCl_2$ and zoniporide (CAS no. 241800-98-6) were purchased from Sigma-Aldrich, (Rehovot, Israel). Insulin 100 U/ml medical grade solution was purchased from Hadassah Medical Center. Isoflurane was obtained from the Authority for Biological and Biomedical Models of the Hebrew University.

Surgical procedure

Animals were anesthetized with isoflurane using a gas anesthesia system (Somnosuite, Kent Scientific, Torrington, CT, USA) at 3.5% and 340 mL/min of room air for induction and 2.9% isoflurane for maintaining anesthesia during the surgical procedure. After obtaining a negative pedal pain reflex, the surgery began, and the heart was exposed. Aortic cannulation was performed *in vivo*, as previously described [1]. Briefly, 200 IU heparin were injected to the left ventricle to prevent blood coagulation and 0.1 mL of 0.5 mol/L KCl was injected to the right atrium to achieve cardiac arrest. A loose knot of 3-0 silk suture was then placed around the ascending aorta. Cannulation was performed *in situ* with a 22 G intravenous catheter (Model: 381323, BD Medical, Franklin Lakes, NJ, USA). This was followed by suture tightening. The heart was then disconnected from the surrounding viscera and connected to the perfusion system *via* the catheter. Upon initiation of perfusion with warm buffer at 7.5 mL/min, the heart began beating spontaneously. The NMR tube with the beating heart were fixed and inserted into the bore of the spectrometer making sure the heart was at the center of the NMR probe.

Perfusion system

The perfusion system was made of medical grade extension tubes and the experimental media were circulated with a peristaltic pump (Masterflex L/S Economy Variable-Speed Drive model 07554-95, Cole-Parmer, Vernon Hills, IL, USA). Thin polyether ether ketone (PEEK) lines (id. 0.040", Upchurch Scientific, Inc., Oak Harbor, WA, USA) were used for media to and from the NMR tube. The inflow line was connected to the intravenous catheter with a homemade adapter. The temperature of the perfusion medium inside the NMR spectrometer during circulation was 37–37.5 °C and was measured continuously and simultaneously with the NMR recordings using an NMR compatible temperature probe (Osensa, Burnaby, BC, Canada).

Intracellular acidification with an NH_4Cl *pre-pulse and an NHE1 blocker*

NH4Cl pre-pulse is a well-established method for inducing intracellular acidification by adding and subsequently removing NH4Cl after a few minutes [2]. This technique leads to intracellular acidification using the equilibrium between ammonium and ammonia [2]. In the isolated heart, this technique can lead to a reduction of the cytosolic pH by 0.2 units, with further decrease when applied in the presence of an NHE1 inhibitor [3]. Briefly, in the first step, the organ is perfused with medium that contains NH_4Cl. Ammonia, at 1.5% of the NH_4Cl concentration at a pH of 7.4, diffuses into the intracellular space through the plasma membrane because it is electrically neutral. However, the ammonium ion cannot cross the membrane and remains in the perfusion buffer. At first, the cytosolic pH becomes alkaline, but with time (~15 minutes) it returns to the normal value and the ammonia-to-ammonium ratio equilibrates. This step is called the pre-pulse. At the second step, NH_4Cl is removed from the perfusion medium, and this causes the ammonia to diffuse out of the cell, leaving hydronium ions trapped in the cell, which leads to a low pH_i. This leads to a pulse of intracellular acidification, as described in Figure S1. From first principles, it is likely that ammonia diffuses across intracellular organelle membranes as well and that the same process occurs therein.

NHE1 accounts for approximately 60% of the proton removal capability of cardiac cells during intracellular acidification [4]. NHE1 on the plasma membrane co-transports H^+ out of the cytosol and Na^+ into the cytosol. Previously, it was shown that inhibition of NHE1 during an NH_4Cl pre-pulse led to a pH drop of 0.5 units in the isolated heart and reduced the pH_i recovery rate [3]. Of note, NHE1 is positioned in an opposite direction in the inner mitochondrial membrane, *i.e.* it co-transports H^+ into the inner mitochondrial matrix and Na^+ out of the mitochondrial matrix and into the cytosol [5]. These reverse NHE1 actions are summarized in Figure S2.

Reducing the activity of NHE1 has been a target for therapy of multiple heart conditions such as heart failure, hypertrophy, and ischemia-reperfusion injury. To this end, several NHE1 inhibitors have been developed such as cariporide, eniporide, and zoniporide, of which, the latter is the most potent and selective [6]. Zoniporide was used here to reduce the pH_i to a level that is lower than what would be achieved using the NH_4Cl pre-pulse alone. The IC_{50} of zoniporide is 14 nM [6] and it was administered here at a concentration of 1 µM, therefore, we may assume a complete inhibition of NHE1.

A possible caveat is that the use of NHE1 could potentially affect other cellular processes that may have additional effects on LDH and PDH. For this reason, we used a zoniporide dose that completely inhibited NHE1 activity but did not induce intracellular acidification when applied alone (without the NH_4Cl pre-pulse). In this way, other pH regulators were able to regulate the pH_i which provided a control for the possible effects of zoniporide itself.

NMR spectroscopy

^{31}P and ^{13}C NMR spectroscopy were performed in a 5.8 T high resolution NMR spectrometer (RS2D, Mundolsheim, France), using a 10 mm broad-band NMR probe. ^{31}P spectra of thermal equilibrium phosphate signals were acquired with a nutation angle of 50° and a repetition time of 1.1 s. The probe was tuned back and forth from ^{31}P to ^{13}C during the experiment to support the requirement of the experimental workflow, in which several injections of hyperpolarized media were performed into the same perfused heart, and the pH and the energy status were monitored using ^{31}P spectroscopy before, in between, and after the injections (Figure 3, main text). Homogeneity optimization (shim) was performed using the water signal on the ^{1}H channel and using the lock system.

Hyperpolarized ^{13}C spectroscopy

Hyperpolarized ^{13}C data were acquired using product-selective saturating-excitation pulses [7] by applying 2.5 ms cardinal sine (Sinc) pulses. Selective excitations of [1-^{13}C]lactate and [^{13}C]bicarbonate were applied consecutively at 6 s intervals (Figure 3, main text), resulting in a 12 s interval for each metabolite. For [1-^{13}C]lactate detection, the selective Sinc pulse was centered at the [1-^{13}C]pyruvate hydrate frequency (179.4 ppm) which resulted in signal intensity ratio (ρ_{lac}) of 0.091 for the C_1 signals of [1-^{13}C]pyruvate to [1-^{13}C]lactate. For [^{13}C]bicarbonate detection, the selective Sinc pulse was centered at 157.7 ppm, which is 214 Hz down-field to the [^{13}C]bicarbonate signal (161.1 ppm). This resulted in a signal intensity ratio (ρ_{bic}) of 0.168 for the C_1 signal of [1-^{13}C]pyruvate to [^{13}C]bicarbonate. The [1-^{13}C]lactate and [^{13}C]bicarbonate signals were fully sampled and depolarized following the application of the respective hyperpolarized product selective saturating-excitation pulses, as described previously [7].

DNP spin polarization and dissolution

Spin polarization and fast dissolution were carried out in a dDNP spin polarization device (HyperSense, Oxford Instruments Molecular Biotools, Oxford, UK) operating at 3.35 T. Microwave frequency of 94.110 GHz was applied for the polarization of the [1-^{13}C]pyruvic acid formulation at 1.45 to 1.55 K. The formulations consisted of 11.1 to 14.0 mmol/L OX063 radical in the neat acid. The dissolution medium consisted of TRIS-phosphate buffer (4 mL) which contained 11.2 mmol/L NaH_2PO_4, 38.8 mmol/L Na_2HPO_4, 33 mmol/L TRIS, and 2 mmol/L HCl. This medium composition was adjusted such that upon addition of 28.5 mg [1-^{13}C]pyruvic acid formulation (in the dissolution phase) the pH of the resulting solution will be 7.4. Prior to the administration of medium to the heart, the hyperpolarized medium (4 mL) ejected from the dDNP device was quickly mixed with a well oxygenated solution, that was designed to complement the hyperpolarized dissolution medium such that the injected medium to the heart will be with a composition that is as close as possible to the perfusion medium. The final volume of the medium perfusing the heart during the hyperpolarized injections with 14 mmol/L hyperpolarized [1-^{13}C]pyruvate was 26 mL. The final composition of the injected medium (after mixing) contained 4.7 mM KCl, 1.2 mM $MgSO_4$, 70 mM NaCl, 25 mM $NaHCO_3$, 1.2 mM KH_2PO_4, 10 mM Glucose, 1.2 mM $CaCl_2$, and 72 U/L insulin. In Groups 5 and 6, 1 µM of zoniporide was added as well. The injection of the resulting hyperpolarized [1-^{13}C]pyruvate solution to the isolated heart was done using a continuous flow setup [8] such that the heart perfusion was not interrupted or altered at any point during the experiment and the hyperpolarized medium was administered at a known flow rate and duration.

Tissue wet weight

At the end of the experiment, the heart was disconnected from the perfusion system, lightly dried with tissue paper, and then weighed to evaluate the tissue wet weight.

LDH and PDH rate calculation

Using product selective saturating-excitation pulses [7], the hyperpolarized metabolites, [1-^{13}C]lactate and [^{13}C]bicarbonate, were fully sampled (and depolarized) by each selective pulse, and only newly synthetized metabolites were detected on each excitation. To calculate the corresponding metabolite production level, [1-^{13}C]pyruvate signal was used as a reference. As we have used a continuous perfusion protocol, the [1-^{13}C]pyruvate concentration in the NMR tube is dynamic and changing according to three phases: increasing – wash in; plateauing to a maximal concentration of 14 mM;

and decreasing - wash-out. The metabolic production rates were calculated only during the time frame when the hyperpolarized [1-^{13}C]pyruvate concentration was constant, (and therefore known). To be able to determine the time points in which the [1-^{13}C]pyruvate concentration was maximal and constant, we used Equation S1 to correct for signal decay due to T_1 relaxation and RF pulses. For each injection, we determined an effective relaxation constant (T_{eff}) that displayed these flow characteristics (Figure 3B, black triangles, main text). The average T_{eff} of all the injections (n=15 hearts, 45 injections) was found to be 41.4 ± 4.3 s.

$$S_{Pyr\_corr}(t) = \frac{S_{Pyr}(t)}{e^{\left(-\frac{t}{T_{eff}}\right)}} \qquad \text{Eq. S1}$$

where $S_{Pyr\_corr}(t)$ is the corrected signal at each time point; $S_{Pyr}(t)$ is the [1-^{13}C]pyruvate signal at each time point; and T_{eff} is the effective relaxation constant (influenced by T_1 and the experienced RF pulses at each specific experiment).

The data points selected for analysis of metabolic conversion rates from each time course were the first four time points which showed a signal that was no less than 10% percent of the maximal corrected [1-^{13}C]pyruvate signal ($S_{Pyr_{corr}}(t)$).

Equation S2 was used to calculate the metabolic conversion rate in µmol/s units in the time points selected for analysis,

$$\upsilon_{product}(t) = \frac{\rho \times V_p}{TR} \times \frac{S_{product}(t)}{S_{pyr}(t)} \times [Pyr] \qquad \text{Eq. S2}$$

where $\upsilon_{product}(t)$ is the production rate of [1-^{13}C]lactate or [^{13}C]bicarbonate at each time point in µmol/s; ρ is the selective pulse excitation ratio which is 0.091 for [1-^{13}C]pyruvate to [1-^{13}C]l lactate and 0.168 for [1-^{13}C]l pyruvate to [^{13}C]bicarbonate; V_p is the volume of the sensitive region of the NMR probe (1.375 mL); TR is the repetition time (12 s); $S_{product}(t)$ is the signal of the product ([1-^{13}C]lactate or [^{13}C]bicarbonate) at each time point; and [Pyr] is the concentration of hyperpolarized [1-^{13}C]pyruvate in the administered medium (14 mM). In the text, the production rate values were multiplied 1,000-fold and the production rates were reported in nmol/s units.

pH_i calculation

^{31}P NMR was used to measure pH_i changes by observing the chemical shift of the intracellular inorganic phosphate (Pi) with reference to the chemical shift of phosphocreatine (PCr) [9]. This was done for the experiments in Groups 4-6, where Pi was not added to the perfusion KH buffer and the Pi signal was therefore solely intracellular. The conversion of the Pi signal chemical shift values to pH values was performed with reference to the chemical shift of PCr using Equation S3 [9],

$$\mathrm{pH} = \mathrm{pKa} + \log\frac{[\Delta\delta(\mathrm{Pi}-\mathrm{PCr}) - \delta\ \mathrm{free\ acid}]}{[\delta\ \mathrm{free\ base} - \Delta\delta(\mathrm{Pi}-\mathrm{PCr})]} \qquad \text{Eq. S3}$$

where $\Delta\delta$ is the chemical shift difference, the pKa is 6.72, δ free base is 5.69, and δ free acid is 3.27, as previously described [10]. The non-linearity between the chemical shift scale and the pH scale was corrected according to Lutz *et al*. [10]. Due to inhomogeneity in pH distribution, a weighted mean pH was used in the analysis as previously described [11].

ATP and PCr content quantification

The ATP and PCr content were calculated from the γ-ATP signal and the PCr signal of the isolated heart in the thermal equilibrium ^{31}P spectra. The quantification was done by comparing this signal to an ATP standard sample acquired on the same experimental day, that contained 111 mM ATP. The difference in the number of acquisitions was considered. A correction for partial saturation during the steady state acquisition was performed using Equation S4.

$$\mathrm{M_0} = \mathrm{M_z}(\alpha, \mathrm{T_1})\frac{\left(1-\cos\alpha\cdot e^{-\frac{\mathrm{TR}}{\mathrm{T_1}}}\right)}{\left(1-e^{-\frac{\mathrm{TR}}{\mathrm{T_1}}}\right)} \qquad \text{Eq. S4}$$

where $\mathrm{M_z}(\alpha, \mathrm{T_1})$ is the actual signal and $\mathrm{M_0}$ is the corrected signal considering partial saturation. The flip angle, α, was 50° and the TR was 1.1 s. The $\mathrm{T_1}$ of ATP and PCr at pH of 7.4 was taken as 1.2 s and 6.1 s, respectively, based on a previous study in the same magnetic field [12].

Normalization of the enzymatic rates to ATP content

It is well established that cardiac tissue deterioration over time is observed under perfusion with crystalloid buffers such as KH buffer. A previous study has shown a reduction of 5-10 % per hour in cardiac contractility [13], and we have previously observed a reduction rate of 10.8 % per hour in ATP content [8]. As LDH and PDH rates were measured three times for each heart, over a time course of a few hours, the decrease in viability could lead to misinterpretation of the data. In addition, the surgical preparation could affect the initial condition of the isolated mouse heart, leading to variability in the starting viability of the hearts under investigation. To overcome this innate variability in viability, the LDH and PDH rates were normalized to the ATP content of each heart, prior to each enzymatic activity determination. This content was obtained from ^{31}P NMR spectra acquired 22.5 min immediately prior to each hyperpolarized [1-^{13}C]pyruvate injection. Figure S4 demonstrates the gain in reproducibility and information of the enzymatic activity determinations using this normalization to the ATP content.

Measurement of DO

DO in the buffer was measured by O_2 sensor spots, (Sticker type: Pst7-10), with an NMR compatible fiber optics DO meter (PreSens, Precision Sensing GmbH, Germany). DO was monitored at two positions within the perfusion system, inside the inflow line, (which perfuses the heart with KH buffer), and inside the NMR tube, in proximity to the isolated heart. The sensors were calibrated with double distilled water bubbled with 100% N_2. Temperature compensation was done with an NMR compatible temperature probe (Osensa, Burnaby, BC, Canada), that was placed in proximity to the O_2 sensor inside the NMR tube. DO was measured every 10 s and recorded using the PreSens software, (Measurement Studio 2 v3.0.1.1413, PreSens GmbH). To calculate the myocardial O_2 consumption (MVO_2), knowledge of the coronary blood flow is required [14]. Since this could not be determined in the perfused heart inside an NMR tube, we monitored the differences in DO between the supply line to the heart (the inflow) and the sensor that was placed in the NMR tube next to the heart. This represented the DO difference that resulted from the heart's O_2 consumption, considering several other parameters as described below.

On each experimental day, the constant difference between the inflow's DO and the NMR tube's DO was determined prior to connecting the heart to the perfusion system. This difference was subtracted from the DO difference that was attributed to the heart's activity. This constant difference is most likely due to evaporation of DO that may vary in various parts of the perfusion system (referred to as R, see Equation S5).

$$R = DO_{inflow\_without\_heart} - DO_{NMR\_without\_heart} \quad \text{Eq. S5}$$

where, $DO_{inflow\_without\_heart}$ and $DO_{NMR\_without\_heart}$ are the respective DOs that were measured in the inflow line and in the NMR tube, respectively, before introducing the heart.

We note that in this system, only one channel could be recoded at a time. Therefore, the DO monitoring was switched between the two DO probes (inflow and NMR tube). First the inflow and the NMR probes were monitored prior to the connection of the heart. Then only the NMR tube was monitored throughout. Several inflow measurements were carried out as well during the experiment as a control for system stability, for each study, but these were very sparse and minimal.

To control for possible DO variations during buffer replacements, the DO characteristics of the inflow line during buffer replacement was characterized independently (n = 3 experiments, 2 buffer replacements in each, without an isolated heart connected to the system). This investigation was done by replacing the buffer that was perfused into the NMR tube in a timeline and process that simulated the NH_4Cl pre-pulse. This simulation showed that the DO increased in the inflow line at the time of buffer switch by up to *ca.* 3% (Figure S5A, Supporting Information). The averaged pattern of the changes in DO in the inflow line during the buffer switch was termed P(t) and is shown in Figure S5. P(t) was included in the calculation of the DO difference that was attributed to the heart's activity as shown in Equation S6,

$$\Delta DO(t) = DO_{inflow\_with\_heart\_baseline} + P(t) - DO_{NMR\_with\_heart}(t) - R \qquad \text{Eq. S6}$$

where ΔDO(t) is the DO difference that is due to the heart's activity at each time point, $DO_{inflow\_with\_heart\_baseline}$ is an average value of the first three points measured in the inflow line, 20 min prior to starting the experimental condition (with the heart connected to the perfusion system), and $DO_{NMR\_with\_heart}(t)$ is the DO that was measured in the NMR tube, with the heart connected to the perfusion system. Further information is provided in Figure S5.

Retrograde perfused heart staining and analysis

The staining procedures were performed as previously described by Bohl *et al.* [15]. Briefly, at the end of the perfusion experiment, the heart was perfused with 4.2 mL of 0.005% (weight/volume) EBV in saline. The intact heart was then wrapped in cling film, placed in an Eppendorf vial, and then stored at -20 °C for no more than 1 h. The heart was then manually cut into 6-7 parallel short-axis sections, using a razor blade on a cold surface. The heart slices were then immersed in freshly prepared 1% (weight/volume) TTC in saline for 3 min at room temperature, and then for 15 min at 37 °C. The slices were then placed in 10% neutral-buffered formalin for 90 min. Each slice was then weighed separately and photographed from both sides.

Viability quantification was performed using the image analysis software ImageJ (NIH, Bethesda, MD) by contouring the differently colored subsets: Blue, area of perfused myocardium (AOP); Red, area at risk (AAR); White, area of necrosis (AON). The relative areas of these subsets were obtained using a pixel count tool. The three subsets were determined by averaging the percent area per slice from the two sides of each section and then correcting for slice weight.

Data analysis and statistics

Spectral processing was performed using MNova (Mestrelab Research, Santiago de Compostela, Spain). Denoising of the hyperpolarized ^{13}C spectra was done as described previously [11] using a low-rank approximation of the MR spectrum in the frequency domain according to Brender *et al.* [16].

Student's *t*-tests were performed with Excel (Microsoft, Ra'anana, Israel). Multiple comparisons were performed with one-way analysis of variance (ANOVA) with repeated measures and with Fisher's Least Significant Difference (LSD). These tests were performed with GraphPad Prism (San Diego, CA, USA).

References

1. Jian Z, Chen YJ, Shimkunas R, et al. In vivo cannulation methods for cardiomyocytes isolation from heart disease models. *Plos One.* 2016;11(8):16.
2. Boron WF, Deweer P. Intracellular pH transients in squid giant-axons caused by CO2, NH3, and metabolic-inhibitors. *J Gen Physiol.* 1976;67(1):91-112.
3. Hartmann M, Decking UK. Blocking Na^+-H^+ exchange by cariporide reduces Na^+-overload in ischemia and is cardioprotective. *J Mol Cell Cardiol.* 1999;31(11):1985-1995.
4. Vaughan-Jones RD, Villafuerte FC, Swietach P, Yamamoto T, Rossini A, Spitzer KW. pH-Regulated Na(+) influx into the mammalian ventricular myocyte: the relative role of Na(+)-H(+) exchange and Na(+)-HCO Co-transport. *Journal of cardiovascular electrophysiology.* 2006;17 Suppl 1:S134-s140.
5. Ruiz-Meana M, Garcia-Dorado D, Pina P, Inserte J, Agullo L, Soler-Soler J. Cariporide preserves mitochondrial proton gradient and delays ATP depletion in cardiomyocytes during ischemic conditions. *American Journal of Physiology-Heart and Circulatory Physiology.* 2003;285(3):H999-H1006.
6. Tracey WR, Allen MC, Frazier DE, et al. Zoniporide: A potent and selective inhibitor of the human sodium-hydrogen exchanger isoform 1 (NHE-1). *Cardiovasc Drug Rev.* 2003;21(1):17-32.
7. Harris T, Uppala S, Lev-Cohain N, et al. Hyperpolarized product selective saturating-excitations for determination of changes in metabolic reaction rates in real-time. *NMR Biomed.* 2020;33(2):e4189.
8. Shaul D, Azar A, Sapir G, et al. Correlation between lactate dehydrogenase/pyruvate dehydrogenase activities ratio and tissue pH in the perfused mouse heart: A potential noninvasive indicator of cardiac pH provided by hyperpolarized magnetic resonance. *NMR Biomed.* 2021;34(2):e4444.
9. Bailey IA, Williams SR, Radda GK, Gadian DG. Activity of phosphorylase in total global ischaemia in the rat heart. A phosphorus-31 nuclear-magnetic-resonance study. *Biochem J.* 1981;196(1):171-178.
10. Lutz NW, Le Fur Y, Chiche J, Pouyssegur J, Cozzone PJ. Quantitative in vivo characterization of intracellular and extracellular pH profiles in heterogeneous tumors: A novel method enabling multiparametric pH analysis. *Cancer Res.* 2013;7:4616.
11. Shaul D, Grieb B, Sapir G, et al. The metabolic representation of ischemia in rat brain slices: A hyperpolarized ^{13}C magnetic resonance study. *NMR Biomed.* 2021:e4509.
12. Nardi-Schreiber A, Gamliel A, Harris T, et al. Biochemical phosphates observed using hyperpolarized ^{31}P in physiological aqueous solutions. *Nat Commun.* 2017;8(1):341.
13. Sutherland FJ, Hearse DJ. The isolated blood and perfusion fluid perfused heart. *Pharmacol Res.* 2000;41(6):613-627.
14. Edlund A, Wennmalm A. Oxygen-consumption in rabbit Langendorff hearts perfused with a saline medium. *Acta psychiatrica Scandinavica.* 1981;113(1):117-122.
15. Bohl S, Medway DJ, Schulz-Menger J, Schneider JE, Neubauer S, Lygate CA. Refined approach for quantification of in vivo ischemia-reperfusion injury in the mouse heart. *American Journal of Physiology-Heart and Circulatory Physiology.* 2009;297(6):H2054-H2058.
16. Brender JR, Kishimoto S, Merkle H, et al. Dynamic imaging of glucose and lactate metabolism by C-13-MRS without hyperpolarization. *Sci Rep.* 2019;9.